ACS OMEGA

Article

Cite This: ACS Omega 2018, 3, 17287−17294

http://pubs.acs.org/journal/acsodf

Accumulation and Subcellular Localization of Acteoside in Sesame Plants (*Sesamum indicum* L.)

Yushiro Fuji, Takashi Ohtsuki, and Hiroshi Matsufuji*

Department of Food Bioscience and Biotechnology, College of Bioresource Sciences, Nihon University, 1866 Kameino, Fujisawa, Kanagawa 252-0880, Japan

Supporting Information

ABSTRACT: The localization of acteoside and its precursors in different organs of sesame plant (*Sesamum indicum* L.), including roots, stems (epidermis, cortex, and stele), leaves (blades and petioles), flower petals, and seeds (immature and mature) was investigated. The highest acteoside content was found in leaf blades (12.3% dry weight), followed by in petioles (3.1%) and petals (2.7%) and at a trace levels or not detected in other organs. In contrast, the known precursors of acteoside, cinnamate, *p*-coumarate, caffeate, tyramine, tyrosol, salidroside, L-3,4-dihydroxyphenylalanine, dopamine, and hydroxytyrosol were not detected in any organs, even by multiple-reaction monitoring analysis by liquid chromatography−electrospray ionization tandem mass spectrometry, despite acteoside being present at high levels in the leaves. The leaves stained with diphenylborinic acid 2-aminoethyl ester (DPBA), producing the acteoside−DPBA complex that was detected by fluorescence at an excitation wavelength of 365 nm, showed accumulation of acteoside at the veins and glandular trichomes. For the first time, the leaf blade organ was shown to contain a large amount of acteoside in the sesame plant, with acteoside synthesis in the leaf petioles and/or blades and accumulation in the glandular trichomes with transport through the veins. However, tyrosine and phenylalanine contents were very low with no downstream metabolites or known acteoside precursors detected in any organs.

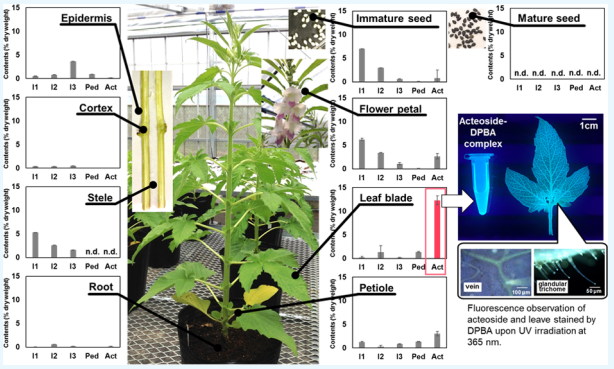

INTRODUCTION

Sesame plants (Pedaliaceae family, *Sesamum indicum* L.) are grown in the tropical or subtropical regions for their seeds, which are one of the world's most important oil crops. The seeds have been well studied for their sesame-specific lignans, such as sesamin and sesamolin, and their chemical composition and functional properties.[1,2] In contrast, very little information is available on the composition of the other organs of sesame because cultivation has primarily been for seed production; the other parts, while large in quantity, are agricultural by-products.[3] Recently, dried powder of young sesame leaves from plants grown to a height of 30−70 cm (about 40−60 days after planting) was commercially produced as a health food supplement in Japan. In previous reports, we showed that young sesame leaves contain three iridoids and eight polyphenols, and among them, acteoside shows strong antioxidant activity and accumulation in the leaves during growth. The acteoside content reached a maximum of 12.9% of dry weight content in leaves at the 4th stage (plant height, 74.5 ± 9.7 cm), which is one of the highest levels reported in plants in nature (Figure 1).[4,5]

Acteoside, also called verbascoside, is widely distributed in dicotyledonous plants, which include over 150 plant species belonging to 20 families and 77 genera.[6] It is not specific to any plant organ, being present in plant roots, bark, stems, leaves, flowers, and fruits,[7] and it shows different localization to other organs of different plants. For example, in *Echinacea pallida*, acteoside was shown to accumulate in flowers more than in leaves and roots.[8] In *Plantago major*L., the acteoside content was highest in flower stalks (2.30 mg g^{-1} DW; 0.23%) followed by seeds (2.28 mg g^{-1}), young leaves (0.02 mg g^{-1}), and old leaves (0.006 mg g^{-1}).[9] Although there are no comprehensive reports on the distribution of acteoside in *S. indicum* L., Potterat et al.[10] isolated acteoside from the root bark of *Sesamum angolense* (Pedaliaceae family) and Grąbkowska et al.[11] reported that the acteoside and isoacteoside contents were higher in leaves and stems than in roots in *Harpagophytum procumbens* (Pedaliaceae family).

Recent pharmacological studies of acteoside have shown extensive biological activities, such as antioxidant,[12] anti-inflammatory,[13] and hepatoprotective activity,[14] in addition to protective properties against neurological diseases, such as Alzheimer's[15,16] and Parkinson's diseases.[17] Therefore, acteoside is expected to be useful for pharmaceutical applications, but commercial-scale production remains unattainable because of the requirements for large-scale evidence-based human

Received: October 14, 2018
Accepted: December 3, 2018
Published: December 13, 2018

DOI: 10.1021/acsomega.8b02798
ACS Omega 2018, 3, 17287−17294

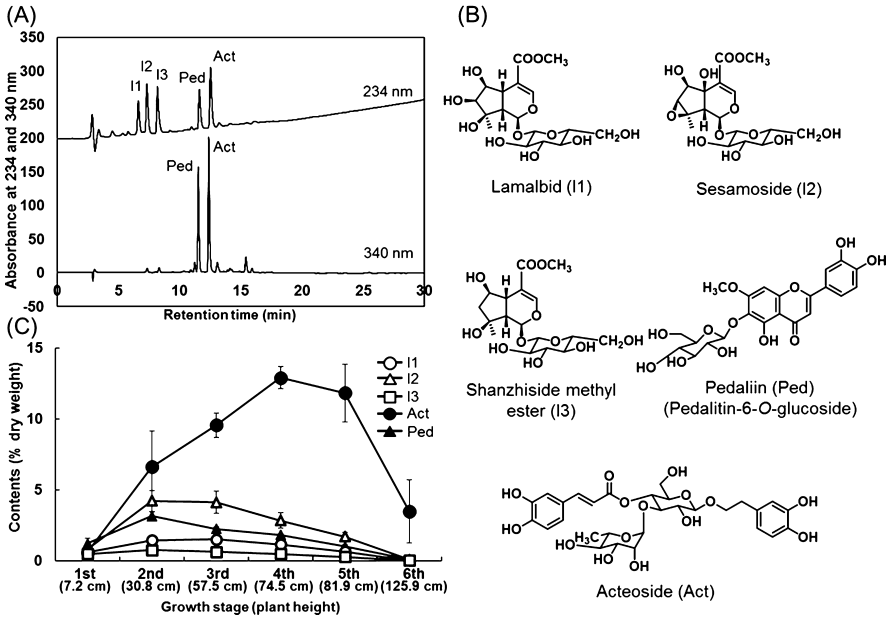

Figure 1. Chemical characterization of sesame leaves and changes in the major compound content at different growth stages. (A) Representative HPLC chromatogram of sesame leaves. (B) Chemical structures of polyphenols and iridoids in sesame leaves. (C) Changes in content at different growth stages.[5]

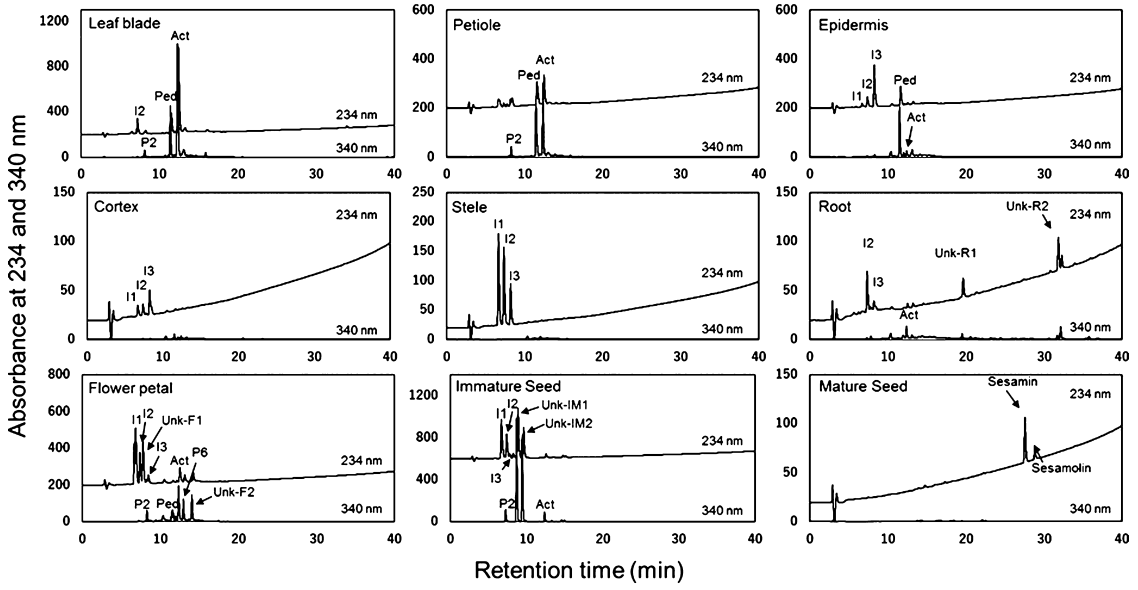

Figure 2. HPLC chromatograms of 60% MeOH extracts from different organs of the sesame plant. I1, lamalbid; I2, sesamoside; I3, shanzhiside methyl ester; P2, chlorogenic acid; Ped, pedaliin; Act, acteoside; and P6, isoacteoside.

studies. Extractions from plant sources have very low yield because of the low content in plants (about 0.02−0.4% in most plants, rarely ∼3.0%), variability in the plant growth conditions, losses in the purification steps to remove contaminants, and so on. On the other hand, a complete chemical synthesis of acteoside has been developed,[18,19] but the complex 15-step procedure required due to the specific structure of acteoside also results in a low yield of 4.4−7.1%. Recently, some biotechnological approaches using nongenetically modified plant cell cultures have been reported,[20,21] but effective mass production and development of efficient cells have not yet been achieved because acteoside biosynthesis, several downstream metabolites, key enzymes, and their corresponding genes remain to be identified and incorporated into this system.

Sesame plants have enormous biosynthetic potential for producing pharmaceutically valuable acteoside and may therefore be an attractive bioproduction resource. In this study, we clarified the distribution of acteoside and its precursors in different organs of the sesame plant to gain basic information on acteoside biosynthesis. Further, subcellular localization of acteoside by fluorescence imaging with diphenylborinic acid 2-aminoethyl ester (DPBA) was examined. Our findings may provide information that will lead to the use of sesame leaves as natural sources of acteoside and may be helpful for elucidating acteoside biosynthesis in sesame plants.

DOI: 10.1021/acsomega.8b02798
ACS Omega 2018, 3, 17287−17294

Table 1. Contents (% DW) of Major Polyphenols and Iridoids in Different Organs of the Sesame Plant[a]

	organ								
	leaf		stem			root	flower	seed	
compounds	blade	petiole	epidermis	cortex	stele	root	petal	immature	mature
Iridoid									
lamalbid	0.27 ± 0.20	1.29 ± 0.10	0.52 ± 0.01	0.34 ± 0.03	5.31 ± 0.02	0.06 ± 0.01	6.23 ± 0.20	7.04 ± 0.03	
sesamoside	1.37 ± 1.31	0.33 ± 0.28	0.80 ± 0.01	0.35 ± 0.01	2.63 ± 0.01	0.57 ± 0.01	3.40 ± 0.03	2.98 ± 0.02	
shanzhiside methyl ester	0.15 ± 0.08	0.86 ± 0.04	3.65 ± 0.01	0.51 ± 0.01	1.65 ± 0.03	0.19 ± 0.01	1.09 ± 0.20	0.62 ± 0.04	
Polyphenol									
chlorogenic acid	0.15 ± 0.05	0.19 ± 0.01	0.03 ± 0.01	tr.			0.35 ± 0.07	0.23 ± 0.01	
pedaliin	1.37 ± 0.13	1.34 ± 0.08	0.91 ± 0.03	tr.			tr.	tr.	
acteoside	12.3 ± 0.97	3.07 ± 0.48	0.15 ± 0.03	tr.		0.13 ± 0.05	2.66 ± 1.70	0.84 ± 0.60	
isoacteoside	0.82 ± 0.15	0.38 ± 0.03	0.28 ± 0.04	tr.	tr.	tr.	0.59 ± 0.38	tr.	

[a]Mean ± standard deviation (SD; n = 9); tr. <0.003%. Blanks are "not detected". Cinnamate, p-coumarate, caffeate, tyrosol, salidroside, and hydroxytyrosol were not detected in all organs.

Table 2. Contents (μg g^{-1} DW) of Free Amino Acids and Amines in Different Organs of the Sesame Plant[a]

	organ								
	leaf		stem			root	flower	seed	
compounds	blade	petiole	epidermis	cortex	stele	root	petal	immature	mature
Amino Acid									
alanine	121.4 ± 2.4	68.3 ± 1.5	47.2 ± 0.6	15.6 ± 0.5	46.8 ± 2.1		227.3 ± 10.4	345.8 ± 4.5	29.6 ± 1.1
arginine	40.6 ± 2.7	32.4 ± 2.7	7.0 ± 0.1	4.0 ± 1.0	7.0 ± 0.1	4.0 ± 0.9	103.6 ± 0.6	315.4 ± 2.9	62.0 ± 5.1
aspartic acid	1167 ± 28.3	141.6 ± 1.6	78.6 ± 0.9	22.4 ± 1.2	93.4 ± 3.8		378.1 ± 9.9	916.6 ± 15.6	151.0 ± 2.0
cysteine							19.3 ± 0.2	19.4 ± 0.3	
glutamic acid	1645.6 ± 41.3	279 ± 7.9	243.4 ± 8.1	85.9 ± 1.8	249.6 ± 8.4	5.8 ± 0.1	672.3 ± 30.4	1934.1 ± 25.2	373.9 ± 5.1
glycine	tr.	tr.	tr.	tr.	tr.	tr.	22.7 ± 0.3	32.8 ± 0.6	tr.
histidine	3.1 ± 0.1	tr.	2.1 ± 0.9		13.9 ± 1.5		231.5 ± 8.3	64.7 ± 3.6	18.6 ± 0.2
isoleucine	37.6 ± 1.4	11.1 ± 0.8			18.8 ± 0.7		103.7 ± 1.3	93.6 ± 0.8	22.2 ± 0.2
leucine	62.0 ± 1.6	38.1 ± 0.5	tr.		5.2 ± 0.1		178.7 ± 4.9	230.6 ± 7.0	24 ± 1.7
lysine	75.5 ± 3.5	37.2 ± 2.1	4.9 ± 0.8		18.0 ± 3.1		122.4 ± 4.1	191.6 ± 3.5	13.6 ± 0.8
methionine	tr.	tr.			tr.		20.3 ± 1.0	43.8 ± 3.0	tr.
phenylalanine	25.9 ± 2.6	5.4 ± 1.0		tr.	tr.		214.5 ± 9.1	103.6 ± 3.1	37.4 ± 1.1
proline	54.4 ± 1.4	18.8 ± 0.7	16.1 ± 0.1	10.6 ± 0.7	15.7 ± 0.6	9.9 ± 0.6	4025.0 ± 32.1	168.2 ± 6.8	20.7 ± 0.2
serine	200.2 ± 4.3	107.4 ± 1.6	29.1 ± 1.4	2.8 ± 0.6	32.2 ± 1.5	1.7 ± 1.2	218.1 ± 49.4	452.0 ± 12.4	15.4 ± 0.7
threonine	120.6 ± 4.4	31.9 ± 0.4	12.7 ± 0.7	3.5 ± 0.1	22.6 ± 1.2		126.7 ± 7.9	168.8 ± 2.3	7.1 ± 0.1
tyrosine	10.2 ± 2.7	tr.	tr.		tr.		63.8 ± 2.1	122.6 ± 5.8	14.5 ± 3.2
valine	65.5 ± 0.4	23.3 ± 1.7			17.5 ± 0.1		209.4 ± 3.0	169.2 ± 3.6	24.2 ± 0.5
GABA	357.5 ± 58.3	234.9 ± 3.1	45.7 ± 1.5				192.6 ± 8.4	1387.3 ± 33.4	tr.
Amine									
tyramine									
L-DOPA									
dopamine									

[a]Mean ± SD (n = 9); tr. <0.5 μg g^{-1}. Blanks are "not detected".

RESULTS

Distribution of Acteoside and Related Compounds in Different Organs. First, we examined the distribution of acteoside and its related compounds in different organs of the sesame plant. Figure 2 shows the representative high-performance liquid chromatography (HPLC) chromatograms of 60% MeOH extracts from different organs: leaves (blades and petioles), stems (epidermis, cortex, and stele), flower petals, roots, and seeds (immature and mature). Major peaks were detected and identified as lamalbid, sesamoside, shanzhiside methyl ester, chlorogenic acid, pedaliin, acteoside, and isoacteoside based on the comparison of retention times and UV and LC−ESI-MS spectra with authentic or isolated compounds. These compounds were previously found in sesame leaves (blades and petioles) and were present in different organs, although additional unknown peaks were detected in flower petals (Unk-F1 and Unk-F2), roots (Unk-R1 and Unk-R2), and immature seeds (Unk-IM1 and Unk-IM2) but were not identified in this study. Sesamin and sesamolin, but not cinnamate, p-coumarate, caffeate, tyrosol, salidroside, or hydroxytyrosol, which are downstream metabolites derived from tyrosine and phenylalanine by the shikimate pathway, were detected in all organs and even in analysis of multiple-reaction monitoring (MRM) analysis with liquid chromatography−electrospray ionization tandem mass spectrometry (LC−ESI-MS/MS).

The breakdown of the major compounds in different organs is given in Table 1. The leaf blade had the most acteoside (12.3 ± 1.0%), followed by petioles (3.1 ± 0.5%). This composition breakdown was almost in agreement with that of the sesame

DOI: 10.1021/acsomega.8b02798
ACS Omega 2018, 3, 17287−17294

leaves grown in a greenhouse at the College of Bioresource Sciences, Nihon University in 2016.[5] Acteoside was present in low levels in the epidermis of the stem and roots (0.15 ± 0.03 and 0.13 ± 0.05%, respectively) but not in the stele. It was also present in the flower petals (2.7 ± 1.7%) and immature seeds (0.84 ± 0.60%) but not in the mature seeds. Isoacteoside, an isomer of acteoside, showed almost the same distribution as acteoside, although at lower levels than acteoside. Thus, large amounts of acteoside in the leaves are assumed to be synthesized in the leaf petiole and/or blades but not in the stem and roots. Additionally, the breakdown in the flower petals suggested that the acteoside-biosynthesized system other than in the leaves would also exist in the flower petals.

Other iridoids, lamalbid, sesamoside, and shanzhiside methyl ester, were present mainly in stems, flower petals, and immature seeds but with different distribution profiles in each organ: lamalbid and sesamoside were present mainly in immature seeds (7.04 ± 0.03 and 2.98 ± 0.02%, respectively), flower petals (6.23 ± 0.20 and 3.40 ± 0.03%, respectively), and stele (5.31 ± 0.02 and 2.63 ± 0.01%, respectively), while shanzhiside methyl ester was found in the epidermis of the stem (3.65 ± 0.01%). In addition, sesamoside was present in larger amounts in leaf blades than in petioles, but lamalbid and shanzhiside methyl ester were found more so in petioles than in leaf blades. Pedaliin, a flavonoid glycoside, was present in leaf blades (1.37 ± 0.13%), petioles (1.34 ± 0.08%), and epidermis (0.91 ± 0.03%) but was not detectable in other organs.

The free amino acid content as well as the amine precursors of acteoside [tyramine, L-3,4-dihydroxyphenylalanine (L-DOPA), and dopamine] in different organs is summarized in Table 2. The units are expressed as $\mu g\ g^{-1}$ ($1\ \mu g\ g^{-1}$ = 0.0001%). For amino acids, glutamic acid was the major amino acid in various organs (85.9−1934.1 $\mu g\ g^{-1}$), except for root and petals, and proline was dominant in roots (5.8 ± 0.1 $\mu g\ g^{-1}$) and petals (4025.0 ± 32.1 $\mu g\ g^{-1}$). γ-Aminobutyric acid (GABA) was found to be present in higher amounts in immature seeds (1387.3 ± 33.4 $\mu g\ g^{-1}$), leaf blades (357.5 ± 58.3 $\mu g\ g^{-1}$), and petioles (234.9 ± 3.1 $\mu g\ g^{-1}$) than in other organs. However, tyrosine and phenylalanine contents as well as acteoside precursors derived from the shikimate pathway were very low (tr. −122.6 $\mu g\ g^{-1}$ and tr. −214.5 $\mu g\ g^{-1}$, respectively) as expected, and no tyramine, L-DOPA, or dopamine, which are downstream metabolites of tyrosine and phenylalanine, were detected in any organs.

Localization of Acteoside in Leaf Blades. To investigate the localization of acteoside in leaf blades, we first subdivided leaf blades horizontally or vertically and assayed the acteoside content. As a result, no differences were found among subdivided leaf blades (data not shown), suggesting that acteoside is distributed uniformly in whole leaves.

Next, we attempted to determine subcellular localization using a DPBA fluorescence stain method. DPBA (also called Naturstoff reagent or Neu's reagent) reacts with compounds such as flavonoids containing *o*-diphenolic and 5-hydroxy-4-keto groups.[22] Before staining leaf blades with DPBA, the fluorescence responses of the major chemical compounds in sesame leaves were tested against DPBA and compared with those of authentic standards and isolated compounds. As shown in Figure 3, controls, quercetin−DPBA and rutin−DPBA complexes, showed yellow fluorescence in accordance with previous reports.[22−24] Acteoside−DPBA complexes showed sky blue fluorescence upon UV irradiation at 365 nm (maximum excitation (Ex) and emission (Em) wavelengths of 400 and 475 nm), similar to that of the caffeate−DPBA complex (Ex/Em = 390/470 nm) but different from the ultramarine color of the hydroxytyrosol−DPBA complex (Ex/Em = 335/385 nm), suggesting that the caffeoyl unit of acteoside predominantly reacts with DPBA to produce a sky blue fluorescence complex. On the other hand, the pedalitin−DPBA complex shows orange fluorescence upon UV irradiation at 365 nm (Ex/Em = 455/570 nm), while pedaliin−DPBA shows a dark color despite the maximum excitation and emission wavelengths being almost the same, suggesting that the fluorescence intensity of the flavonoid glycoside is weakened compared to that of the aglycone−DPBA complex. No fluorescence was observed in the mixtures of iridoids and DPBA (data not shown). Further, when the mixture of acteoside and pedaliin in the concentration ratio (12:1 w/w) in the leaf blade was reacted with DPBA, the DPBA complex showed sky blue fluorescence (Figure S1). On the basis of these results, the DPBA method could be utilized to examine subcellular localization of acteoside in sesame leaves without the interference of other compounds (iridoids and polyphenols) being in them.

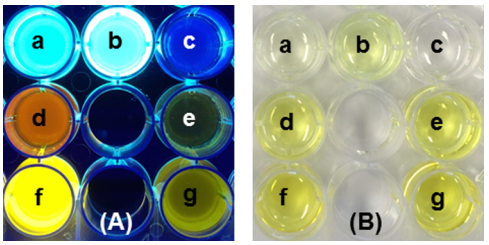

Figure 3. Fluorescence response of DPBA complexes under UV irradiation at 365 nm (A) or visible light (B). (a) Acteoside−DPBA complex. (b) Caffeate−DPBA complex. (c) Hydroxytyrosol−DPBA complex. (d) Pedalitin−DPBA complex. (e) Pedaliin−DPBA complex. (f) Quercetin−DPBA complex. (g) Rutin−DPBA complex.

The sesame leaf blade stained with DPBA after eliminating chlorophyll showed sky blue fluorescence in the whole leaf upon UV radiation at 365 nm, while the leaf blade without DPBA did not show fluorescence (Figure 4A,B). Moreover, fluorescence microscopy observations revealed that sky blue fluorescence occurred in veins and glandular trichomes (Figure 4C,D). Thus, for the first time, acteoside was demonstrated to

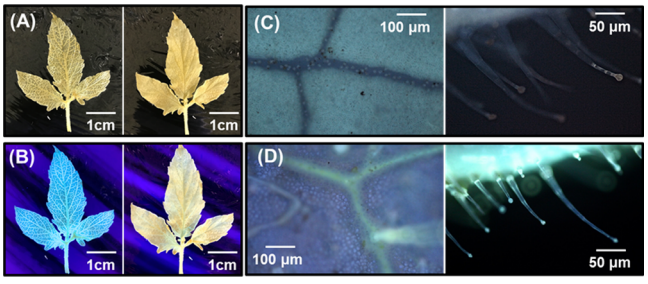

Figure 4. Fluorescence imaging of sesame leaves stained with DPBA. (A) Sesame leaves stained with (left) or without (right) DPBA under visible light. (B) Sesame leaves stained with (left) or without (right) DPBA upon UV irradiation at 365 nm. (C) Microscopic photograph of veins (left) and trichomes (right) under visible light. (D) Fluorescence microscopy photograph of veins (left) and trichomes (right) under UV irradiation at 365 nm.

DOI: 10.1021/acsomega.8b02798
ACS Omega 2018, 3, 17287−17294

pass thorough the veins and accumulate in the glandular trichomes of sesame leaves.

DISCUSSION

To clarify the distribution of acteoside and its related compounds in the sesame plant, exhaustive HPLC or LC−ESI-MS/MS analyses for polyphenols, iridoids, amino acids, and acteoside precursors were performed on all organs of the sesame plant, including leaves (leaf blades and petioles), stems (epidermis, cortex and stele), roots, flower petals, and seeds (immature and mature). Acteoside was present in leaf blades at the highest levels (12.3%), followed by in the petioles (3.1%). Also, fluorescence imaging observation of leaf blades stained with DPBA revealed that acteoside was present in the veins and in the glandular trichomes of leaves. To the best of our knowledge, there is no data for the subcellular localization of acteoside in natural plants and we here demonstrate for the first time that acteoside accumulates in the glandular trichomes of sesame leaves. Thus, one can assume that acteoside in sesame leaves is synthesized in the petioles and/or leaf blades and accumulates in the glandular trichomes following passage through the veins. However, our finding that known acteoside precursors were not found or were detected at low levels in all organs of sesame plants raises the question of how and from which compounds acteoside is biosynthesized.

The three chemical components of acteoside are caffeate, saccharide (glucose and rhamnose), and hydroxytyrosol aglycon. Although the downstream pathway of acteoside biosynthesis remains to be fully elucidated, the components of caffeate and hydroxytyrosol (or salidroside) are known to be biosynthesized from phenylalanine and tyrosine, respectively, which are derived from the shikimate pathway.[25] The caffeoyl moiety of acteoside is biosynthesized from phenylalanine via a cinnamate pathway, whereas the hydroxytyrosol moiety is biosynthesized from tyrosine with tyramine and/or dopamine intermediates (Figure 5). In survey studies, some acteoside

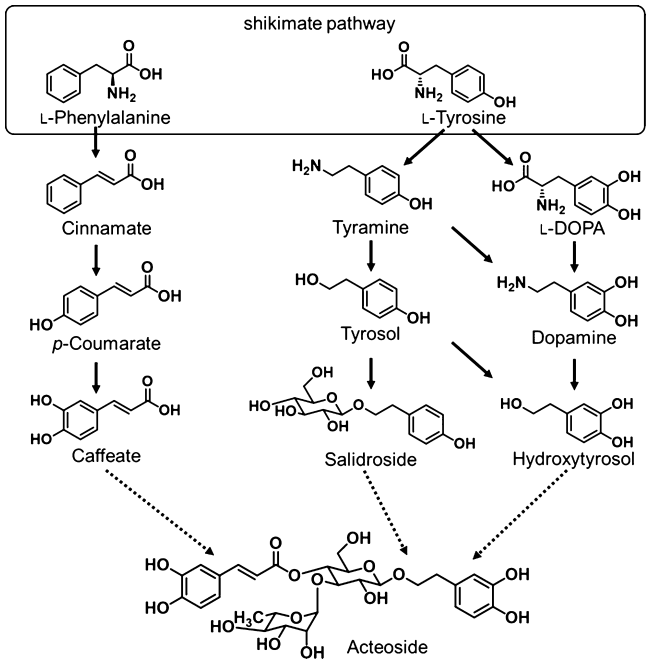

Figure 5. Proposed biosynthesis pathway of acteoside described in previous reports.[25]

precursors such as hydroxytyrosol, tyrosol, *p*-coumarate, caffeate, or hydroxytyrosol glycoside were found in olive fruits[26−28] and lilac flowers,[29] which contain a large amount of acteoside (up to 9.0% in *Coratina* and *Rocciola* olive; less than 3.0% in other olive cultivars; 2.48% in lilac). Despite sesame leaves having accumulated larger amounts of acteoside (about 12%) than olive fruits and lilac flowers, we could not identify acteoside precursors in any organs of sesame plants. Thus, there are two possible explanations for acteoside biosynthesis in sesame plants: one is that synthesis occurs by a new, currently unknown pathway and the other is that key enzymes are activated in the biosynthesis pathway. Further investigation is needed to clarify these possible explanations. So far, Liu et al.[30] reported that production of acteoside increased 2- to 3-fold when a cell suspension culture of *Cistanche salsa* was fed a combination of phenylalanine and tyrosine. To clarify the related genome, several transcriptional studies on acteoside biosynthesis have been conducted on the cultured cells of *Olea europaea*,[31] *Cistanche deserticola*,[32] and *Rehmannia glutinosa*.[33] We plan to examine the production of acteoside by incorporating isotope-labeled amino acids and the major genomic determinants of acteoside biosynthesis in sesame plants using RNA-seq technology in vitro and in vivo.

This and our previous studies show that no acteoside is detected in stele of the stem and provide some support for the hypothesis that the acteoside biosynthesis system in sesame plants is localized in leaf petioles and flower petals. Although acteoside is present in many dicotyledonous plants, the organ of accumulation differs by plant species and the role of acteoside is not fully elucidated. Glandular trichomes accumulate a variety of secondary metabolites, such as terpenes, fatty acid derivatives, alkaloids, and flavonoids, most of which protect the plant from abiotic and biotic stresses.[34,35] Therefore, acteoside also may protect the sesame plant owing to its strong antioxidant activity. However, the extraordinarily high amounts that were found to accumulate in the leaves (12.3% in this study; 12.9% in a previous study) are among the highest levels reported in plants in nature. From the findings that the major polyphenols in sesame leaves were limited to acteoside and pedalitin (pedalitin-6-*O*-glucoside), a flavonoid biosynthesis-related gene may be present at a lower copy number than in other plants, disrupted, or missing, resulting in the accumulation of a large amount of acteoside. Considering another possibility, iridoids were found to be major constituents in leaves in a previous report,[5] and they were present at higher levels in stems, suggesting that they are transported to leaves through the steles of stems. Although the biosynthesis pathways of lamalbid, sesamoside, and shanzhiside methyl ester have been reported,[36] there is no information about the site of iridoid biosynthesis in *S. indicum* L. Further investigation is required to unravel the complexity of the biochemical pathways, such as transcriptome analysis to obtain robust genomic data and identification of the key enzyme.

In summary, we conclude that sesame plants have excellent biosynthetic potential for acteoside. To use this bioproduction resource of pharmaceutically valuable acteoside and sesame plants, further investigation to elucidate the acteoside biosynthesis pathway is needed, such as experiments utilizing isotope incorporation and in vitro and in vivo molecular biological approaches.

DOI: 10.1021/acsomega.8b02798
ACS Omega 2018, 3, 17287−17294

EXPERIMENTAL SECTION

Chemical Reagents. Acteoside was obtained from BP Biochemicals Inc. (San Diego, CA, USA). Pedalitin, pedaliin, lamalbid, sesamoside, and shanzhiside methyl ester were isolated previously.[5] Hydroxytyrosol, DPBA, chloral hydrate, glycerol, and amino acid mix standard (consisting of 17 amino acids) were obtained from Sigma-Aldrich Co. (St. Louis, MO, USA). Caffeate, quercetin, rutin, and GABA were from Wako Chemical Industries (Osaka, Japan). AccQ•Tag Ultra precolumn derivatization kit including borate buffer and AQC derivatizing reagent were from Waters Co. (Milford, MA, USA). All regents were used without further purification.

Plant Materials. The sesame plants (*S. indicum* L. variety Myanmar Black Sesame) were cultivated in a greenhouse at the College of Bioresource Sciences, Nihon University in June 2017 as described in our previous report.[5] Fresh leaves, stems, roots, and petals were collected at about 80 days after planting (plant height, about 70 cm; $n = 9$). The leaf blades and petioles from leaves and the epidermis, cortex, and stele from stems were separated manually and collected. Immature (white) and mature (black) seeds were collected at about 80−90 days (plant height, 70−90 cm; $n = 9$) and about 90−110 days (plant height, 120−150 cm; $n = 9$) after planting, respectively. The plant organs are illustrated in Figure S2. After collection, organ samples were immediately frozen in liquid nitrogen, lyophilized, and ground using a mortar and pestle and then kept at −20 °C until analysis. On the other hand, fresh leaf samples ($n = 3$) for fluorescence observation were collected from plants with a height of about 70 cm and immediately stained with DPBA as described below.

Polyphenol, Iridoid, and Acteoside Precursor Analysis. Polyphenol and iridoid analyses were performed in accordance with methods described in our previous study.[5] In this study, the available aromatic precursors of acteoside (cinnamate, *p*-coumarate, caffeate, tyrosol, salidroside, and hydroxytyrosol), sesamin, and sesamolin were analyzed under the same conditions. In brief, each dried organ (about 25 mg) was extracted twice with 1 mL of 60% MeOH in a sonicating bath (15 min, room temperature). The extracts were filtered through a 0.22 or 0.45 μm PVDF membrane filter and analyzed with HPLC and/or LC−ESI-MS/MS. HPLC was conducted using a Shimadzu Prominence system (Kyoto, Japan) with a photodiode array detector and a Waters XBridge C18 column (4.6 × 150 mm, 5 μm) and eluted with a linear MeCN gradient in 0.1% HCOOH (5−35% MeCN in 15 min, 35−100% MeCN in 25 min, and 100−5% MeCN in 1 min) at a flow rate of 0.8 mL min^{-1} at 40 °C. The sample injection volume was 10 μL, and the eluent was monitored at 234 and 340 nm. For LC−ESI-MS/MS, a Waters Quattro Premier XL mass spectrometer was coupled to an ACQUITY UPLC system. The compounds were separated on an ultraperformance liquid chromatography system with a Waters HSS T3 column (2.1 × 50 mm, 1.7 μm) and a linear MeCN gradient in 0.1% HCOOH (5−35% MeCN in 3 min, 35−100% MeCN in 5 min, and 100−5% MeCN in 1 min) at a flow rate of 0.3 mL min^{-1} at 40 °C. The ion source conditions were optimized as follows: negative electrospray ionization; source temperature, 150 °C; capillary voltage, 3.5 kV; desolvation temperature, 500 °C; flow rate of desolvation gas, 1000 L h^{-1}; and flow rate of cone gas, 50 L h^{-1}. For MRM experiments to detect aromatic precursors of acteoside, specific transitions of parent and product ions were monitored as shown in Figure S3. Calibration curves were constructed using authentic or isolated compounds (0.5−250 nmol mL^{-1}). The amount of each analyzed compound in the organs was expressed as percentage of dry organ weight.

Amino Acid and Amine Analysis. Seventeen amino acids, GABA, and available amine precursors of acteoside (tyramine, L-DOPA, and dopamine) in different organ samples were analyzed by LC−ESI-MS/MS after derivatization with 6-aminoquinolyl-*N*-hydroxysuccinimidyl carbamate (AQC) using a Waters AccQ•Fluor reagent kit according to the manufacturer's instructions. In brief, each dried organ (about 25 mg) was extracted twice with 1 mL of ultrapure water in a sonicating bath (15 min). The water extracts were filtered through a 0.22 μm PVDF membrane filter and directly used for derivatization. Aliquots (10 μL) of both extracts or the standard solution were mixed with 70 μL of AccQ•Tag borate buffer and 20 μL of AQC reagent. After heating at 55 °C for 10 min to finalize the derivatization reaction, 1 μL of the sample was injected into the LC−ESI-MS/MS system with a Waters AccQ•Tag Ultra column (2.1 × 100 mm, 1.7 μm). The applied solvent system consisted of eluent (A), which is a specified dilution of Waters AccQ•Tag Ultra Eluent A, and eluent (B), which is Waters AccQ•Tag Ultra Eluent B. The column temperature was set to 55 °C, and gradient elution was applied with a flow rate of 0.7 mL min^{-1} as follows: 0−0.54 min, 0.1% B; 0.54−5.74 min, 0.1−9.1% B; 5.74−7.74 min, 9.1−21.2% B; 7.74−8.04 min, 21.2−59.6% B; 8.04−8.05 min, 59.6−90% B; 8.05−8.64 min, 90−90% B; 8.64−8.73 min, 90−0.1% B; and 8.73−9.50 min, 0.1−0.1% B. For MRM experiments, monitoring specific transitions of parent and product ions are summarized in Table S1. The amount of each analyzed compound in the organs was expressed as μg of g-dry organ weight.

Fluorescence Spectra of Selected Compounds with DPBA. The fluorescence derivatization method was performed according to a previous report[22] with some modifications. The mixture (1.5 mL) in 50% dimethyl sulfoxide (DMSO) solution containing isolated compounds (10 μM in the final of lamalbid, sesamoside, shanzhiside methyl ester, acteoside, pedaliin, or pedalitin) or positive control (10 μM of quercetin or rutin) and DPBA (100 μM) were incubated at room temperature for 10 min under dark conditions. Primary fluorescence of the mixture was observed with the naked eye under UV irradiation (365 nm) using a transilluminator, and excitation and emission spectra of the mixture were obtained on a JASCO FP-6500 spectrofluorometer.

Fluorescence Microscopy of Sesame Leaf Tissue Stained with DPBA. Leaf organs were fixed according to previous reports[37,38] with some modifications. Fresh sesame leaves were immersed in ethanol containing 10% acetic acid for 24 h at room temperature, followed by sequential 20 min soaks in 90, 50, and 30% ethanol. After rinsing with water, the leaves were exposed to a clearing reagent (8 g chloral hydrate, 1 mL glycerol, and 2 mL water) for 1 h to remove chlorophyll. After rinsing with water again, the leaves were stained in 1 mM DPBA-DMSO solution for 10 min. The stained leaf tissue was observed under a fluorescence microscope with a U-MNU (365 nm) exciter filter (Olympus BX51, Olympus, Tokyo, Japan).

DOI: 10.1021/acsomega.8b02798
ACS Omega 2018, 3, 17287−17294

■ ASSOCIATED CONTENT

Supporting Information

The Supporting Information is available free of charge on the ACS Publications website at DOI: 10.1021/acsomega.8b02798.

Fluorescence response of the DPBA complex when the mixture of acteoside and pedaliin in the concentration ratio (12:1 w/w) in the leaf blade was reacted with DPBA; illustration of different organs in the sesame plant used in this study; MRM chromatograms of acteoside and its related compounds; and MRM conditions of free amino acids and amine precursors of acteoside (tyramine, L-DOPA, and dopamine) (PDF).

■ AUTHOR INFORMATION

Corresponding Author

*E-mail: hmatsufu@brs.nihon-u.ac.jp.

ORCID

Hiroshi Matsufuji: 0000-0001-9190-1434

Notes

The authors declare no competing financial interest.

■ ACKNOWLEDGMENTS

We are grateful to Prof. Satoshi Kubota of the Department of Agricultural Bioscience, College of Bioresource Sciences, Nihon University for valuable discussions and technical support in the cultivation of *S. indicum* L. We are also thankful to the General Research Institute of Nihon University for LC−ESI-MS/MS measurements. This study was financially supported by the Nihon University President Grant Initiative and JSPS KAKENHI Grant Number JP15K12247.

■ REFERENCES

(1) Namiki, M. The chemistry and physiological functions of sesame. *Food Rev. Int.* **2009**, *11*, 281−329.

(2) Wan, Y.; Li, H.; Fu, G.; Chen, X.; Chen, F.; Xie, M. The relationship of antioxidant components and antioxidant activity of sesame seed oil. *J. Sci. Food Agric.* **2015**, *95*, 2571−2578.

(3) Liu, L.; Liu, J.; Li, H.; Zhang, H.; Liu, J.; Zhang, H. Equilibrium, kinetic, and thermodynamic studies of lead (II) biosorption on sesame leaf. *BioResources* **2012**, *7*, 3555−3572.

(4) Matsufuji, H.; Ohmori, J.; Goto, S.; Chino, M.; Wada, E.; Uchida, A.; Fukahori, K.; Yamagata, K.; Sakurai, H. Radical scavenging activity of polyphenols in young leaves of *Sesamumindicum* L. *Nippon Shokuhin Kagaku Kogaku Kaishi* **2011**, *58*, 88−96.

(5) Fuji, Y.; Uchida, A.; Fukahori, K.; Chino, M.; Ohtsuki, T.; Matsufuji, H. Chemical characterization and biological activity in young sesame leaves (*Sesamumindicum* L.) and changes in iridoid and polyphenol content at different growth stages. *PLoS One* **2018**, *13*, No. e0194449.

(6) He, J.; Hu, X.-P.; Zeng, Y.; Li, Y.; Wu, H.-Q.; Qiu, R.-Z.; Ma, W.-J.; Li, T.; Li, C.-Y.; He, Z.-D. Advanced research on acteoside for chemistry and bioactivities. *J. Asian Nat. Prod. Res.* **2011**, *13*, 449−464.

(7) Jiménez, C.; Riguera, R. Phenylethanoid glycosides in plants: structure and biological activity. *Nat. Prod. Rep.* **1994**, *11*, 591−606.

(8) Cheminat, A.; Zawatzky, R.; Becker, H.; Brouillard, R. Caffeoyl conjugates from *Echinacea* species: structures and biological activity. *Phytochemistry* **1988**, *27*, 2787−2794.

(9) Zubair, M.; Nybom, H.; Lindholm, C.; Rumpunen, K. Major polyphenols in aerial organs of greater plantain (*Plantago major* L.), and effects of drying temperature on polyphenol contents in the leaves. *Sci. Hortic.* **2011**, *128*, 523−529.

(10) Potterat, O.; Msonthi, J. D.; Hostettmann, K. Four iridoid glucosides and a phenylpropanoid glycoside from *Sesamum angolense*. *Phytochemistry* **1988**, *27*, 2677−2679.

(11) Grąbkowska, R.; Mielicki, W.; Wielanek, M.; Wysokińska, H. Changes of phenylethanoid and iridoid glycoside distribution in various tissues of shoot cultures and regenerated plants of *Harpagophytum procumbens* (Burch.) DC. ex Meisn. *S. Afr. J. Bot.* **2014**, *95*, 159−164.

(12) Xiong, Q.; Kadota, S.; Tani, T.; Namba, T. Antioxidative effects of phenylethanoids from *Cistanche deserticola*. *Biol. Pharm. Bull.* **1996**, *19*, 1580−1585.

(13) Seo, E. S.; Oh, B. K.; Pak, J. H.; Yim, S.-H.; Gurunathan, S.; Kim, Y.-P.; Lee, K. J. Acteoside improves survival in cecal ligation and puncture-induced septic mice *via* blocking of high mobility group box 1 release. *Mol. Cells* **2013**, *35*, 348−354.

(14) Jing, W.; Chunhua, M.; Shumin, W. Effects of acteoside on lipopolysaccharide-induced inflammation in acute lung injury via regulation of NF-κB pathway in vivo and in vitro. *Toxicol. Appl. Pharmacol.* **2015**, *285*, 128−135.

(15) Korshavn, K. J.; Jang, M.; Kwak, Y. J.; Kochi, A.; Vertuani, S.; Bhunia, A.; Manfredini, S.; Ramamoorthy, A.; Lim, M. H. Reactivity of metal-free and metal-associated amyloid-β with glycosylated polyphenols and their esterified derivatives. *Sci. Rep.* **2015**, *5*, 17842.

(16) Shiao, Y.-J.; Su, M.-H.; Lin, H.-C.; Wu, C.-R. Acteoside and isoacteoside protect amyloid-β peptide induced cytotoxicity, cognitive deficit and neurochemical disturbances *in vitro* and *in vivo*. *Int. J. Mol. Sci.* **2017**, *18*, 895.

(17) Yuan, J.; Ren, J.; Wang, Y.; He, X.; Zhao, Y. Acteoside binds to caspase-3 and exerts neuroprotection in the rotenone rat model of Parkinson's disease. *PLoS One* **2016**, *11*, No. e0162696.

(18) Duynstee, H. I.; de Koning, M. C.; van der Marel, G. A.; van Boom, J. H. Synthesis of verbascoside: A dihydroxyphenylethyl glycoside with diverse bioactivity. *Eur. J. Org. Chem.* **1999**, 2623−2632.

(19) Kawada, T.; Asano, R.; Hayashida, S.; Sakuno, T. Total synthesis of the phenylpropanoid glycoside, acteoside. *J. Org. Chem.* **1999**, *64*, 9268−9271.

(20) Gómez-Aguirre, Y. A.; Zamilpa, A.; González-Cortazar, M.; Trejo-Tapia, G. Adventitious root cultures of *Castilleja tenuiflora* Benth. as a source of phenylethanoid glycosides. *Ind. Crops Prod.* **2012**, *36*, 188−195.

(21) Georgiev, M.; Ludwig-Müller, J.; Weber, J.; Stancheva, N.; Bley, T. Bioactive metabolite production and stress-related hormones in Devil's claw cell suspension cultures grown in bioreactors. *Appl. Microbiol. Biotechnol.* **2010**, *89*, 1683−1691.

(22) Matteini, P.; Agati, G.; Pinelli, P.; Goti, A. Modes of complexation of rutin with the flavonoid reagent diphenylborinic acid 2-aminoethyl ester. *Monatsh. Chem.* **2011**, *142*, 885−893.

(23) Peer, W. A.; Brown, D. E.; Tague, B. W.; Muday, G. K.; Taiz, L.; Murphy, A. S. Flavonoid accumulation patterns of transparent testa mutants of *Arabidopsis*. *Plant Physiol.* **2001**, *126*, 536−548.

(24) Lee, J. H.; Kim, Y.; Hoang, M. H.; Jun, H.-j.; Lee, S.-J. Rapid quantification of cellular flavonoid levels using quercetin and a fluorescent diphenylboric acid 2-amino ethyl ester probe. *Food Sci. Biotechnol.* **2014**, *23*, 75−79.

(25) Alipieva, K.; Korkina, L.; Orhan, I. E.; Georgiev, M. I. Verbascoside - A review of its occurrence, (bio)synthesis and pharmacological significance. *Biotechnol. Adv.* **2014**, *32*, 1065−1076.

(26) Ryan, D.; Robards, K. Critical Review. Phenolic compounds in olives. *Analyst* **1998**, *123*, 31R−44R.

(27) Machado, M.; Felizardo, C.; Fernandes-Silva, A. A.; Nunes, F. M.; Barros, A. Polyphenolic compounds, antioxidant activity and l-phenylalanine ammonia-lyase activity during ripening of olive cv. "Cobrançosa" under different irrigation regimes. *Food Res. Int.* **2013**, *51*, 412−421.

(28) Alagna, F.; Mariotti, R.; Panara, F.; Caporali, S.; Urbani, S.; Veneziani, G.; Esposto, S.; Taticchi, A.; Rosati, A.; Rao, R.; Perrotta, G.; Servili, M.; Baldoni, L. Olive phenolic compounds: metabolic and

DOI: 10.1021/acsomega.8b02798
ACS Omega 2018, 3, 17287−17294

transcriptional profiling during fruit development. *BMC Plant Biol.* **2012**, *12*, 162.
(29) Tóth, G.; Barabás, C.; Tóth, A.; Kéry, Á.; Béni, S.; Boldizsár, I.; Varga, E.; Noszál, B. Characterization of antioxidant phenolics inSyringa vulgarisL. flowers and fruits by HPLC-DAD-ESI-MS. *Biomed. Chromatogr.* **2015**, *30*, 923−932.
(30) Liu, J.-Y.; Guo, Z.-G.; Zeng, Z.-L. Improved accumulation of phenylethanoid glycosides by precursor feeding to suspension culture of *Cistanche salsa*. *Biochem. Eng. J.* **2007**, *33*, 88−93.
(31) Saimaru, H.; Orihara, Y. Biosynthesis of acteoside in cultured cells of Olea europaea. *J. Nat. Med.* **2009**, *64*, 139−145.
(32) Li, Y.; Wang, X.; Chen, T.; Yao, F.; Li, C.; Tang, Q.; Sun, M.; Sun, G.; Hu, S.; Yu, J.; Song, S. RNA-seq based de novo transcriptome assembly and gene discovery of *Cistanche deserticola* fleshy stem. *PLoS One* **2015**, *10*, No. e0125722.
(33) Wang, F.; Zhi, J.; Zhang, Z.; Wang, L.; Suo, Y.; Xie, C.; Li, M.; Zhang, B.; Du, J.; Gu, L.; Sun, H. Transcriptome analysis of salicylic acid areatment in *Rehmannia glutinos*a hairy roots using RNA-seq technique for identification of genes involved in acteoside biosynthesis. *Front. Plant Sci.* **2017**, *8*, 787.
(34) Valkama, E.; Salminen, J.-P.; Koricheva, J.; Pihlaja, K. Changes in leaf trichomes and epicuticular flavonoids during leaf development in three birch taxa. *Ann. Bot.* **2004**, *94*, 233−242.
(35) Thitz, P.; Possen, B. J. H. M.; Oksanen, E.; Mehtätalo, L.; Virjamo, V.; Vapaavuori, E. Production of glandular trichomes responds to water stress and temperature in silver birch (*Betula pendula*) leaves. *Can. J. For. Res.* **2017**, *47*, 1075−1081.
(36) Alipieva, K.; Kokubun, T.; Taskova, R.; Evstatieva, L.; Handjieva, N. LC-ESI-MS analysis of iridoid glucosides in *Lamium* species. *Biochem. Syst. Ecol.* **2007**, *35*, 17−22.
(37) Tattini, M.; Di Ferdinando, M.; Brunetti, C.; Goti, A.; Pollastri, S.; Bellasio, C.; Giordano, C.; Fini, A.; Agati, G. Esculetin and esculin (esculetin 6-O-glucoside) occur as inclusions and are differentially distributed in the vacuole of palisade cells in *Fraxinus ornus* leaves: A fluorescence microscopy analysis. *J. Photochem. Photobiol., B* **2014**, *140*, 28−35.
(38) Villani, T. S.; Koroch, A. R.; Simon, J. E. An improved clearing and mounting solution to replace chloral hydrate in microscopic applications. *Appl. Plant Sci.* **2013**, *1*, 1300016.

DOI: 10.1021/acsomega.8b02798
ACS Omega 2018, 3, 17287−17294